RSC Advances

RSC Advances

www.rsc.org/advances

ROYAL SOCIETY
OF CHEMISTRY

www.rsc.org/advances

Tuning Interaction of Immiscible Poly(L-lactide)/Poly(vinylidene fluoride) Blend by Adding Poly(methyl methacrylate) via a Competition Mechanism and the Resultant Mechanical Properties

Hai-ming Chen[1], Xiong-fei Wang[1], Dan Liu[1], Yang-peng Wang[1], Jing-hui Yang[1], Yong Wang[1*],

Chao-liang Zhang[2], Zuo-wan Zhou[1]

1. Key Laboratory of Advanced Technologies of Materials (Ministry of Education), School of Materials Science & Engineering, Southwest Jiaotong University, Chengdu, 610031, China

2. State Key Laboratory of Oral Diseases, Sichuan University, Chengdu, 610041, China

ABSTRACT: In this work, a mutually miscible third polymer, i.e. poly(methyl methacrylate) (PMMA), was introduced into an immiscible poly(L-lactide) (PLLA)/poly(vinylidene fluoride) (PVDF) (60/40, wt/wt) blend. The interactions, between PMMA and both components of the immiscible blend, were first theoretically predicated by calculating the interfacial tensions and then experimentally proved by characterizing the glass transition and crystallization behaviors of the components. The results showed that although PMMA was miscible to PLLA and PVDF, it exhibited stronger interaction to PVDF and had a tendency to merge together with PVDF component during the melt-compounding processing. There was a competition effect between PLLA and PVDF when they absorbed PMMA. Consequently, the interaction between PVDF and PLLA was enhanced by the bridge effect of PMMA. Furthermore, the migration and diffusion of PMMA carried a part of PLLA component into PVDF component (or carried PVDF component into PLLA component), forming so called occlusion structure. The mechanical properties were measured and the results showed that at appropriate PMMA contents (20-30 wt%), the ternary blends exhibited excellent fracture toughness. The enhanced interaction between components and the formation of the occlusion structure were suggested to be the main toughening mechanisms. This work demonstrated that the microstructure and mechanical properties of the immiscible polymer blends could be tuned by adding a mutually miscible third polymer via a competition mechanism, therefore, it provided an alternative strategy to prepare the microstructure/property-controllable materials.

---
* Corresponding author: Tel: +86 28 87603042;
E-mail: yongwang1976@163.com

1. INTRODUCTION

Polymer blending is believed to be one of the most efficient ways to prepare new high-performance materials. While some polymer blends are completely miscible at the molecular level, most blends are immiscible. The immiscible polymer blends usually exhibit multiple phase structure, such as sea-island, co-continuous, layer by layer and salami-like, etc. The final chemical and physical properties of the immiscible polymer blends are greatly dependent upon the morphology that is formed during the sample preparation process. For example, polymer blends with sea-island morphology usually exhibit excellent comprehensive mechanical properties. The representative blends are rubber toughening system.[1-4] If the blends exhibit co-continuous morphology, they may combine the properties of both components in a favorable way.[5] Such morphology is usually fabricated when preparing the conductive polymer composites. In this condition, the selective location of conductive fillers in one component of the blend is favorable to greatly reduce the percolation threshold of conductive fillers.[6-8] The layer by layer structure, which can be well fabricated through the co-extrusion processing method, is usually fabricated to improve the gas barrier properties of the blends.[9-12] The salami-like structure, although it is difficult to be fabricated during the simple melt-compounding processing, exhibits potential ability to improve the fracture toughness of the immiscible polymer blends.[13-16]

It is well known that the morphology of immiscible polymer blends is influenced by many factors, including weight ratio, interaction between components, viscosity ratio and processing conditions such as temperature and shear stress, etc.[17] Among these factors, interaction between components is one of the most important parameters, because it influences not only the morphology evolution of the blends during the melt-processing but also the stress transferring between components under the load condition, affecting directly the fracture behavior of the blends.[18-20] Improving the interaction between components of the immiscible polymer blend is then the key issue while preparing the high-performance materials.

The classical strategy to improve the interaction between components of the immiscible polymer blends is introducing a compatibilizer, including block and/or graft copolymer that usually has the similar chain structure with each component of the blends[21, 22] and the third component that is

2

miscible with each component of the blends.[23] During the melt-compounding process, the compatibilizer tends to selectively locate at the interface between components and lower the interfacial tension, which makes the morphology change easier. The most apparent change is the dramatic decrease of the dispersed component size.[22] Furthermore, it has been widely reported that the presence of the compatibilizer also facilitates the fabrication of salami-like structure in the immiscible polymer blends.[14,24] For example, Dong W.Y. et al. [14] introduced ethylene glycidylmethacrylate-graft-styrene-co-acrylonitrile (EGMA-g-AS) into poly(L-lactide) (PLLA)/polyamide 11 (PA11) and found that premixing PLLA and EGMA-g-AS resulted in the typical salami-like structure for the final material with many very small domains of PA11 dispersed in the PLLA component, which endowed the material with excellent fracture toughness. However, Zhang H.S. et al.[24] found that the formation of the salami-like structure was also dependent upon the interaction between compatibilizer and the components of the immiscible polymer blends. They introduced respectively poly(styrene-ethylene/butyldiene-styrene) (SEBS) and maleic anhydride-grafted SEBS (SEBS-g-MA) into poly(ethylene terephthalate) (PET)/linear low density polyethylene (LLDPE) and found that the SEBS-g-MA compatibilized PET/LLDPE blends could show the salami-like structure at high content of SEBS-g-MA due to the stronger interaction between PET and SEBS-g-MA.

Different from the compatibilizing efficiency of common block or graft copolymers, the addition of a mutually miscible third component has been proved another efficient way to improve the interaction of the immiscible polymer blends.[23,25-29] The morphology of the ternary blend is greatly dependent upon the content of the third polymer. Sometimes the two-phase structure can be preserved to a certain extent[23,25] and in other conditions, a single-phase structure can be achieved for the ternary blend.[26-29] Substantially enhanced interfacial activity, which lowers the interfacial tension and enhances the interfacial adhesion, is believed the main compatibilizing mechanism.[23] As a consequence, an improvement in ultimate mechanical properties can be expected. For example, Lizymol P. P. and Thomas S. introduced poly(vinyl chloride) (PVC) into the immiscible poly(ethylene-co-vinyl acetate)/poly(styrene-co-acrylonitrile) (EVA/SAN) blends and found that PVC acted as a common solvent for the blends and interacted with either of the components, producing novel sets of miscible systems with good mechanical properties.[30-33] However, it is not very clear whether the salami-like structure can be also fabricated by adding the

mutually miscible third component or not.

Poly(L-lactide) (PLLA) is a biodegradable and biocompatible polyester, and it attracts much attention in recent years because of its excellent strength, modulus and completely renewable resources. Therefore, it has been thought a promising alternative to petroleum-based plastic.[34-36] PLLA-based blends have been widely investigated and among them, the blends of poly(ethylene oxide) (PEO)/PLLA,[37] poly(vinyl acetate) (PVAc)/PLLA,[38,39] and poly(methyl methacrylate) (PMMA)/PLLA,[40, 41] etc, are miscible. Poly(vinylidene fluoride) (PVDF) is an important polymer that exhibits a wide range of application in supercapacitors, transducers, actuators, batteries.[42,43] The miscible PVDF-based blends include PVDF/PMMA,[44] PVDF/acrylic rubber,[45] PVDF/poly(butylene succinate),[46,47] PVDF/poly-3-hydroxybutyrate (PHB),[48] etc. Although the blend of PLLA/PVDF is seldom researched, it is believed that the blend has potentially promising application in many fields. PLLA is immiscible with PVDF in a thermodynamic viewpoint,[49-51] but the two polymers have a mutually miscible third polymer, i.e. PMMA. Therefore, it is believed that PMMA can be used to improve the interaction between PLLA and PVDF and to fabricate a new material with promising properties.

In this work, different contents of PMMA are introduced into PLLA/PVDF blend with a certain composition, at which the blend exhibits the co-continuous structure. The main attention is focused on the interaction and morphological changes in the ternary blends. The mechanical properties are measured to show the microstructure-property relationship of the new material.

2. EXPERIMENTAL PART

2.1 Materials

PLLA (trade name of 2002D, with a D-isomer content of 4.3%, a melt flow rate (MFR) of 4-8 g/10min (190 °C /2.16 kg) and a density of 1.24 g/cm³) was purchased from NatureWorks®, USA. PVDF (trade name of F901, with the MFR of 8.0 g/10min (190 °C /2.16 kg)) was purchased from 3F company, China. PMMA (trade name of CM-211, with the MFR of 16 g/10min (230 °C /3.8 kg) and the density of 1.19 g/cm³) was purchased from Chimei company, China.

2.2 Sample preparation

The pellets of PLLA, PVDF and PMMA were dried at 80 °C for 10 h to erase the effect of moisture. The melt-compounding of the ternary blends was conducted on a twin-screw extruder

SHJ-20 (Nanjing Ruiya, China) at a screw speed of 150 rpm and the melt temperatures of 150-185 °C from hopper to die. After being granulated, the pellets were injection-molded to obtain the standard dumbbell specimens (with a width of 10 mm and a thickness of 4.2 mm) using an injection-molding machine (NISSEI-PS40E5ASE, Japan) at the melt temperatures of 180-185-185 °C from hopper to nozzle and a mould temperature of 20 °C. In the ternary blends, the weight ratio between PLLA and PVDF was maintained at 60/40, and the content of PMMA was varied from 10 to 40 wt%. For making a comparison, the binary blends of PLLA/PVDF (60/40), PLLA/PMMA (60/40) and PVDF/PMMA (50/50) were also prepared through the completely same processing procedures.

2.3 Rheological measurement

The melt viscosity of raw material was measured using a stress controlled rheometer DHR-1 (TA Instrument, USA) at the melt temperature of 185 °C and the frequency sweep from 0.03 to 300 rad/s. The strain amplitude was maintained at 1% and the initial torque was 10 μN·m. The sample disk was prepared through a compression molding way at the melt temperature of 185 °C and a pressure of 5 MPa. The thickness and diameter of the sample disk were 1 and 20 mm, respectively. The measurement was carried out in nitrogen atmosphere. For all the measurements, the samples were tested within the linear viscoelastic strain range, which could be estimated by an initial survey through a dynamic strain sweep experiment at strains ranging from 0.01 to 100%.

2.4 Contact angle measurement

The surface tensions of all the components were deduced by the contact angle measurement, which was carried out on the surfaces of compression-molded films of pure PLLA, pure PVDF and pure PMMA. The compression-molded film had a thickness of 1 mm and a diameter of 20 mm. The pellets were compression-molded at 185 °C to obtain film for testing. Contact angle was measured at 20 °C with a drop shape analysis system DSA 100 (KRÜSS, Germany). Measurement of a given contact angle was carried out for at least 5 times. Double distilled water (H_2O) and methylene iodide (CH_2I_2) with analytical purity were used as probe liquids. The drop volumes for H_2O and CH_2I_2 were 50 and 5 μL, respectively.

2.5 Dynamic mechanical analysis (DMA)

The dynamic mechanical properties were measured using a dynamic mechanical analysis (DMA) Q800 (TA Instrument, USA). The single cantilever mode was selected. A rectangular sample,

which was directly cut from an injection-molded bar, was used and it had a length of 35 mm, a width of 10 mm and a thickness of 4.2 mm. The measurement was carried out from -60 to 140 °C at a heating rate of 3 °C/min and at a frequency of 1 Hz.

2.6 Differential scanning calorimetry (DSC)

The melting behaviors of the samples were investigated using a differential scanning calorimetry (DSC) STA 449C Jupiter (Netzsch, Germany). Sample of about 8 mg, which was cut from an injection-molded bar, was directly heated from 0 ℃ to 200 ℃ at a heating rate of 10 ℃/min. All the measurements were carried out in nitrogen atmosphere.

2.7 Wide angle X-ray diffraction (WAXD)

The crystalline structure of the injection-molded bar was further investigated using a wide angle X-ray diffraction (WAXD) X'pert PRO diffractometer (Panalytical, the Netherlands) with Ni-filtered Cu Kα radiation. The continuous scanning angle range used in this study was from 5° to 40° and the measurement was operated at 40 kV and 40 mA.

2.8 Scanning electron microscopy (SEM)

The phase morphology of the blend was characterized using a scanning electron microscope (SEM) Fei Inspect (FEI, the Netherlands) with an accelerating voltage of 10 kV. Before characterization, the sample was first cryogenically fractured in liquid nitrogen, and then the fractured surface was immersed into the aqueous sodium hydroxide solution with OH^- concentration of 3 mol/L at 80 °C for 3 h to remove PLLA phase. In this condition, aqueous sodium hydroxide solution didn't destroy PVDF phase domain. After that, the treated surface was carefully washed using alcohol and water with the aid of sonication, successively. Finally, after being coated with a thin layer of gold, the treated surface was characterized using SEM.

2.9 Transmission electron microscopy (TEM)

The phase morphology of the blend was also characterized using a transmission electron microscope (TEM) JEM-2100F (JEOL, Japan) with operating voltage of 200 kV. An ultrathin section with a thickness of about 90 nm, which was cut using a cryo-diamond knife on a microtome EM UC6/FC6 (LEICA, Germany), was used for TEM characterization.

2.10 Tensile properties measurement

Tensile properties were measured on an injection-molded bar using a tensile testing machine AGS-J (SHIMADZU, Japan) according to ASTMD 638. The sample had a width of 10 mm and a

thickness of 4.2 mm. During the measurement, the gauge distance was set at 50 mm and a

cross-head speed of 50 mm/min was used. The measurements were mainly carried out at room

temperature (23±1 ℃), and the average value of mechanical properties reported was derived from

at least five specimens.

3. RESULTS AND DISCUSSION

3.1 Determination of the interaction between components

 The interfacial interaction between components in the ternary PLLA/PVDF/PMMA blend can be

well described by the methodology of thermodynamic work of adhesion, which is based on the

calculation of the surface energy of these polymers. Contact angle measurement is a traditional

method applied to calculate the surface energy of solid according to the following relations:[52,53]

$$r_{LV}(1+\cos\theta) = 2\sqrt{r_{SV}^d \cdot r_{LV}^d} + 2\sqrt{r_{SV}^p \cdot r_{LV}^p} \qquad (1)$$

$$r_{SV} = r_{SV}^d + r_{SV}^p \qquad (2)$$

 where θ is the contact angle, subscripts '*LV*' and '*SV*' denote the interfacial liquid-vapor and

surface-vapor tensions, respectively, while the superscripts '*d*' and '*p*' denote the disperse and

polar components of total surface tension, r_{SV}, respectively. Once the surface energy is obtained,

the interfacial energy can be calculated according to the Harmonic-mean equation and

Geometric-mean equation:[54]

Harmonic-mean equation:

$$\gamma_{12} = \gamma_1 + \gamma_2 - 4\left(\frac{\gamma_1^d\gamma_2^d}{\gamma_1^d + \gamma_2^d} + \frac{\gamma_1^p\gamma_2^p}{\gamma_1^p + \gamma_2^p}\right) \qquad (3)$$

and Geometric-mean equation:

$$\gamma_{12} = \gamma_1 + \gamma_2 - 2\left(\sqrt{\gamma_1^d\gamma_2^d} + \sqrt{\gamma_1^p\gamma_2^p}\right) \qquad (4)$$

 where γ_i is the surface energy of component i, γ_i^d, and γ_i^p are the dispersive and polar parts

of the surface energy of component i, respectively.

 Therefore, one can measure the contact angles of some representative liquids on the surface of

polymer. Generally, the selected representative liquids are double distilled water (H_2O) and

methylene iodide (CH_2I_2). According to the literature, the surface energy data of H_2O and CH_2I_2

are γ^p =50.8 mJ/m^2 and γ^d =22.5 mJ/m^2 for H$_2$O, and γ^p =2.3 mJ/m^2 and γ^d =48.5 mJ/m^2 for CH$_2$I$_2$,[55] respectively.

Table 1 shows the contact angles of distilled H$_2$O and CH$_2$I$_2$ on the surfaces of PLLA, PVDF and PMMA films. In this work, the contact angles were measured at room temperature. However, when calculating the surface energy of the component in the melt state (i.e. processing temperature), the influence of high temperature on the surface energy needs to be considered. The temperature coefficients of components investigated in this work can be seen in the literatures and the data are listed in Table 2.[56,57] According to equations (1) and (2), the surface energy data are calculated and the results are also shown in Table 2. Then, the interfacial energies between PVDF and PMMA (PVDF-PMMA) and between PLLA and PMMA (PLLA-PMMA) can be calculated and the results are shown in Table 3. From Table 3 one can see that the interfacial tension of PVDF-PMMA couple is much smaller than that of PLLA-PMMA couple. It indicates that the interaction between PVDF and PMMA is stronger than that between PLLA and PMMA. In other words, if the three polymers are melt-compounded simultaneously, although PMMA is miscible with both PVDF and PLLA, it preferentially merges together with PVDF. Furthermore, the hydrogen bonding interaction between carbonyl (>C=O) of PMMA and methane (>CH$_2$) of PVDF also promotes the migration of PMMA to PVDF.[58]

To well understand the variations of the interactions between components in the ternary blends, the glass transition of each component in the binary blends was first investigated using DMA. Figure 1 exhibits the glass transition of each component in the binary blends of PLLA/PVDF (60/40), PLLA/PMMA (60/40) and PVDF/PMMA (50/50). For the binary PLLA/PVDF blend, the curve exhibits two maxima. The maximum at low temperature (-31 °C) is related to the glass transition of the unrestricted amorphous PVDF component, while the maximum at higher temperature (71 °C) is related to the glass transition of the unrestricted amorphous PLLA component. It is worth noting that the glass transition temperature (T_g), whether for PLLA component (T_{g-PLLA}) or for PVDF component (T_{g-PVDF}), is very similar to that of pure PLLA[59] or pure PVDF.[60] This indicates that the binary PLLA/PVDF blend is immiscible. As expected, either for the binary PLLA/PMMA or for the PVDF/PMMA blend, it exhibits one glass transition

temperature at 85.1 ($T_{g-PLLA/PMMA}$) or 73.9 °C ($T_{g-PVDF/PMMA}$). This agrees well with the

observations reported in the literatures that the binary PLLA/PMMA and PVDF/PMMA blends are

miscible and the blends exhibit only one glass transition temperature. [40,41,44]

The glass transition of each component in the ternary PLLA/PVDF/PMMA blends is shown in

Figure 2. For making a comparison, the mechanical loss factor of the binary PLLA/PVDF (60/40)

blend is also shown. Interestingly, compared with the binary PLLA/PVDF blend, the glass

transitions of both PLLA and PVDF components in the ternary blends are changed apparently

when PMMA is present in the blends, especially at high content of PMMA. There are several

characteristics, which are worthy of noting.

First, T_{g-PVDF} shifts to higher temperatures with the increase of PMMA content. At PMMA

contents of 30 and 40 wt%, T_{g-PVDF} increases up to 10 °C. Obviously, the enhancement of

T_{g-PVDF} is mainly attributed to the presence of PMMA in the ternary blends, whether it is present

in the PVDF component or it locates at the interface between PVDF and PLLA, which restricts the

chain segment motion of PVDF component. Compared with the glass transition temperature of the

binary PVDF/PMMA (50/50) blend (seen in Fig. 1), which exhibits the $T_{g-PVDF/PMMA}$ of 73.9 °C,

it can also be deduced that in the ternary blends, the effect of PMMA on chain segment motion of

PVDF is weakened.

Second, all the ternary blends exhibit the similar T_{g-PLLA} to that of the binary PLLA/PVDF

blend, but the intensity of the $\tan\delta$ of PLLA increases with the increase of PMMA content,

especially at high content of PMMA. Considering the glass transition temperature of the

components in the binary PLLA/PMMA (60/40) blend (seen in Fig. 1), which exhibits the

$T_{g-PLLA/PMMA}$ of 85.1 °C, it can be deduced that the chain segment motion of PLLA in the ternary

blends is possibly not restricted by PMMA. Contrarily, more PLLA chain segments are activated

possibly due to the enhanced interaction between PLLA and PVDF.

Third, the glass transition of PMMA component in the ternary blends also depends on its content.

At relatively low content (10 wt%), the glass transition of PMMA component is difficult to be

differentiated. This indicates that the chain segment motion of PMMA is completely restricted

possibly due to that most of PMMA are present in PVDF component. When the contents of PMMA increase up to 20 and 30 wt%, a shoulder peak is observed at about 95 °C, relating to the motion of greatly influenced PMMA chain segments. Interestingly, for the PLLA/PVDF/PMMA (60/40/40) sample, an isolated glass transition is observed at 105 °C, which is very close to the glass transition of pure PMMA. This indicates that some regions rich in PMMA component are formed in the ternary blend.

It is already proved that, whether for the PVDF/PMMA or for the PLLA/PMMA, the binary blend exhibits only one T_g and the value is between the data of pure PVDF and pure PMMA (or between the data of pure PLLA and pure PMMA) (seen in Fig. 1). Interestingly, from the previous results of the ternary blends, one can see that besides the variations of the glass transitions of both PVDF and PLLA components, the ternary blend containing a high content of PMMA also shows the glass transition of PMMA component and the corresponding T_{g-PMMA} is very close to that of pure PMMA. Furthermore, the glass transition of PLLA becomes stronger with increasing content of PMMA, indicating that more PLLA molecular chains are activated by adding PMMA. More visualized schematic representation about the interactions between components in the ternary blend and the corresponding glass transitions are shown in Figure 3.

The binary PLLA/PVDF blend (Fig. 3a) is immiscible and there is a clear interface between PLLA and PVDF components. Therefore, the glass transition of one component is not affected by the other component. For the ternary PLLA/PVDF/PMMA blend containing low content of PMMA (Fig. 3b), although PMMA tends to merge together with PVDF, it also shows interaction with PLLA component. Consequently, PMMA mainly locates at the interface region or at the PVDF side of the interface. The strong PVDF-PMMA interaction and weak PLLA-PMMA interaction promote some PLLA molecular chains entering into PVDF component, leading to the presence of the shoulder at the left side of the glass transition of PLLA component. In other words, there is a competition effect between PVDF and PLLA when they absorb PMMA component. In this condition, PMMA exhibits a bridge effect to intensify the interaction between PVDF and PLLA. For the ternary blend containing high content of PMMA (Fig. 3c), the interaction between PVDF and PMMA is saturated and the interaction between PLLA and PMMA becomes more apparent. Most likely, the interaction of PLLA-PMMA is comparable to that of PVDF-PMMA. In

this condition, a new interface region that mainly contains PMMA component is formed between PLLA and PVDF. This results in the presence of the glass transition of the isolated PMMA component.

3.2 Crystallization behaviors

The effect of PMMA on the interaction between components in the ternary blends can also be proved by the variations of the crystalline structures of PLLA and PVDF components. Figure 4 shows the WAXD profiles of all the samples investigated in this work. Although PLLA is a semi-crystalline polymer, its crystallization ability is relatively low and usually it is completely amorphous through common processing procedures such as melt-extrusion, injection-molding and compression-molding, etc.[61] However, PVDF shows high crystallization ability and semi-crystalline PVDF can be easily achieved. As shown in Fig. 4, the binary blend exhibits the characteristic diffraction peaks at 2θ=17.8° and 19.9°, attributing to the diffractions of (100) and (110) crystal planes of α-phase PVDF. There is no other apparent diffraction peaks of PLLA in the WAXD profile. This indicates that only PVDF component crystallizes during the cooling process and PLLA component is in the amorphous state. With the presence of PMMA (10 wt%), although a new diffraction peak at 2θ=18.4°, relating to the diffraction of (020) crystal plane of α-phase PVDF, is observed for the ternary blend, the (100) and (110) crystal planes exhibit lower intensity compared with those of the binary blend. This indicates that the presence of PMMA restricts the crystallization of PVDF.[44,62] Further increasing the content of PMMA, the characteristic diffraction peaks of PVDF become inconspicuous and even disappear completely at high contents of PMMA (30 and 40 wt%). In this condition, completely amorphous PVDF component is also achieved in the ternary blends.

Figure 5 shows the DSC heating curves of the binary PLLA/PVDF and the ternary PLLA/PVDF/PMMA blends. For the binary blend, it exhibits several transitions in the heating curve. The transitions at about 57 °C, 107.2 °C and 147.6/154.2 °C are ascribed to the glass transition (T_{g-PLLA}), cold crystallization ($T_{cc-PLLA}$) and melting (T_{m-PLLA}) of PLLA component, respectively. While the endothermic peak at 168.4 °C is related to the fusion of PVDF crystalline structure, which is still very close to the melting point (T_{m-PVDF}) of pure PVDF.[62] This further proves that the binary blend is immiscible. Similarly, the cold crystallization and melting behavior

of PLLA component as well as the melting behavior of PVDF in the ternary blend is greatly affected by PMMA. At a PMMA content of 10 wt%, the ternary blend shows invariant T_{g-PLLA}, $T_{cc-PLLA}$ and T_{m-PLLA}, while the T_{m-PVDF} shifts to lower temperature (166.7 °C) compared with the binary blend. This indicates that the presence of a few PMMA does not affect the crystallization and melting behaviors of PLLA component but affects the crystallization behavior of PVDF component through preventing the lamellar thickening during the crystallization process of PVDF.[44] Possibly, most of PMMA merges together with PVDF. Increasing PMMA content up to 20 wt%, the $T_{cc-PLLA}$ shifts to higher temperatures and the crystallization enthalpy becomes smaller. Specifically, the intensity of the endothermic peaks of PLLA becomes smaller, too. This indicates that the cold crystallization of PLLA component becomes more difficult and fewer PLLA crystallites form during the DSC heating process.[63,64] Furthermore, a weak shoulder at the right side of the main fusion peak of PLLA is observed and the corresponding temperature is about 161.3 °C. Obviously, this is attributed to the fusion of PVDF crystallites with many defects. When PMMA contents increase up to 30 and 40 wt%, the endothermic peak ascribing to the melting of PVDF crystallites disappears completely. According to the previous WAXD results, one can believe that completely amorphous PVDF is achieved in the ternary blends.

3.3 Morphology

Generally, the enhanced interaction between components of the immiscible polymer blends also results in the variation of morphology. Machado J.M. et al.[23] introduced PMMA into immiscible styrene-maleic anhydride (SMA)/acrylonitrile-butadiene-styrene (ABS) blends, in which the two components were miscible with PMMA. They found that the addition of PMMA resulted in less aggregated and more highly dispersed rubber domains in the blend. Similarly, Moussaif N. et al.[25] introduced PMMA into the immiscible polycarbonate (PC)/PVDF blend, in which PMMA was only compatible with PC. More regular and finer phase dispersion was also observed when the PMMA content was higher than 20 wt%. The previous observations indicate that the mutually miscible third component acts as a compatibilizer.

Here, to well understand the morphology of the samples, the melt viscosities of three components were first measured through rheological measurement. The results are shown in Figure 6. One can

see that under the common extrusion-injection molding processing conditions, PMMA exhibits the biggest melt viscosity while PLLA exhibits the smallest one.

Subsequently, the phase morphologies of all the blends were characterized using SEM. The SEM images are shown in Figure 7. From Fig. 7a one can see that the binary PLLA/PVDF blend exhibits the typical two-phase structure, in which the black regions represent PLLA component that was removed during the sample preparation. At higher magnifications, one can see that the residual PVDF component scarcely contains PLLA component, indicating the weak interaction between PLLA and PVDF. Furthermore, the binary blend exhibits a quasi-cocontinuous structure. This mainly results from the combined action of viscosity ratio and volume fraction ratio between PLLA and PVDF. For the ternary blends, since only PLLA can be removed by aqueous sodium hydroxide solution, the residual part observed from SEM image consists of PVDF and PMMA components simultaneously. Therefore, it can be thought as the PVDF-PMMA phase. From Fig. 7b to 7e one can see that the ternary blends exhibit apparently changed morphologies compared with the binary blend. First, the size of the PVDF-PMMA phase increases gradually with increasing PMMA content. Second, the ternary blends exhibit the occlusion structure with many dispersed PLLA particles in the PVDF-PMMA phase. The occlusion structure is similar to the salami-like structure as reported previously. The encapsulated PLLA particles have the average diameter of about 140 nm. Specifically, the more PMMA in the ternary blends, the more the dispersed PLLA particles in the PVDF-PMMA phase are. Obviously, the formation of the occlusion structure is mainly related to the different interactions between components of the ternary blends. The previous results have already shown that although PMMA is miscible with PLLA and PVDF, the interaction between PVDF and PMMA is stronger than that between PLLA and PMMA. During the melt-compounding process, the migration of PMMA to PVDF component inevitably carries some PLLA component into PVDF component.

The morphology of the representative PLLA/PVDF/PMMA (60/40/30) blend was also investigated using TEM. As shown in Figure 8, the ternary blend exhibits quasi-cocontinuous structure as a whole. Furthermore, one can see that besides the occlusion structure with dispersed PLLA particles in the continuous PVDF-PMMA phase, many small dispersed PVDF-PMMA particles (typically 0.1-0.2 μm) can be seen in the continuous PLLA phase, also forming the occlusion structure. It is suggested that the formation of the occlusion structure is mainly related to

13

the presence of PMMA component, which plays the role of carrier and carries PLLA (or PVDF) component into PVDF (or PLLA) component, when PMMA component migrates and diffuses in the melt during the melt-compounding processing.

3.4 Mechanical properties

The enhanced interaction between PLLA and PVDF components and the formation of the occlusion structure, both of them are believed to be favorable for the improvement of the fracture toughness. The representative engineering stress-strain curves of all the samples and the corresponding tensile properties are shown in Figure 9. From the engineering stress-strain curves (Fig. 9a) one can see that all the samples exhibit the similar deformation behaviors and the curves can be classified into several stages: elastic region, yield region, cold-drawing region and fracture. The difference is that adding PMMA leads to the enlargement of the cold-drawing region. Specifically, at PMMA contents of 20-30 wt%, the stress-strain curves even show the strain-hardening region. However, at very high content of PMMA (40 wt%), the sample shows the largely reduced cold-drawing region. The inserted image in Fig. 9a shows the macroscopic appearance of the tensile-fractured samples. It can be seen that at appropriate PMMA contents (20 and 30 wt%), the necking phenomenon of the sample during the tensile process becomes inconspicuous, which indicates that the stress transfer in the sample is very efficient.

The elongation at break and the fracture energy, both of which can be used to represent the fracture toughness of the sample, are shown in Fig. 9b. The binary blend exhibits the elongation at break and fracture energy of about 47.6% and 43.4 J, respectively. Adding 10 wt% PMMA does not change the fracture toughness apparently. However, by adding 20 wt% PMMA, the elongation at break of the ternary blend increases up to 276.7%, which is much higher than that of the binary blend. This clearly indicates that the fracture toughness of the blend is improved by adding PMMA. However, further increasing the content of PMMA results in the decrease of the fracture toughness. For the ternary blend containing 40 wt% PMMA, the elongation at break decreases to 25.1%, which is even smaller than that of the binary blend.

According to the previous results, it can be deduced that there are several possibilities for the toughening of the ternary blends by adding appropriate PMMA contents. The first possibility is mainly related to the enhanced interaction between PLLA and PVDF components, which is achieved by adding appropriate PMMA contents. Under this condition, more PLLA molecular

14

chains are activated on the one hand. On the other hand, the enhanced interaction facilitates the stress transfer between components during the tensile process and avoids the stress concentration at the interface. Generally, the intense stress concentration usually induces the crack initiation and propagation along the interface, leading to the fracture with less energy absorption.

The second possibility is mainly related to the formation of the occlusion structure. From SEM images one can see that the encapsulated PLLA particles in the PVDF-PMMA phase have an average diameter of about 140 nm. Since the modulus of PVDF is much smaller than that of PLLA, it is believed that the well-dispersed PLLA nanoparticles can exhibit the similar toughening mechanism to that of rigid particles in the ductile polymers.[65,66] Similarly, the encapsulated PVDF-PMMA particles in the PLLA phase exhibit the role of a toughening agent, promoting the plastic deformation of PLLA phase under the load condition.

The third possibility is that the decreased crystallization ability of PVDF component induced by PMMA may contribute to the toughening effect. For the binary PVDF/PMMA blend, it has been reported that the addition of PMMA reduces the crystallization ability of PVDF, leading to the decrease of the crystallinity. Therefore, the elongation at break increases with the decrease of PVDF crystallinity. In this work, with the increase of PMMA content, the size of the PVDF-PMMA phase increases gradually. Consequently, the contribution of PVDF-PMMA phase for the enhancement of the ductility becomes more apparent.

However, high content of PMMA does not insure the improvement or the maintenance of the fracture toughness; contrarily, it induces the brittle fracture of the sample. PMMA is a brittle polymer and high content of PMMA makes the PVDF-PMMA phase more brittle. Although the size of the PVDF-PMMA phase is still larger than that of PLLA, the deformation ability of the PVDF-PMMA phase becomes smaller, leading to the brittle fracture of the sample accordingly. Furthermore, as observed from DMA measurement, at very high content of PMMA (40 wt%), due to the competition effect of PLLA and PVDF on PMMA, a part of PMMA locates at the interface and forms a new region that is rich in PMMA component. Although the interactions, which are mainly present between PLLA and PMMA and between PVDF and PMMA, are strong enough, the intermediate region containing PMMA is brittle and it has low ability to transfer the stress. Consequently, the sample becomes brittle again.

The elastic modulus showed in Fig. 9c exhibits that the binary blend and the ternary blend

containing 10 wt% PMMA have high modulus. However, further increasing PMMA content results in the decrease of the modulus. This can be attributed to the morphological changes of the ternary blends induced by PMMA. It is well known that the modulus of the immiscible polymer blend is mainly determined by the matrix property. For the binary blend, it exhibits the quasi-cocontinuous structure and PLLA has larger size compared to PVDF. Consequently, the modulus of the sample is mainly determined by PLLA rather than by PVDF. The addition of 10 wt% PMMA does not apparently change the morphology (Fig. 7); therefore, the ternary blend exhibits the similar modulus to that of the binary blend. However, at high content of PMMA, the size of the PVDF-PMMA phase increases and a part of PLLA component enters into the PVDF-PMMA phase. Consequently, the contribution of PLLA to the modulus of the ternary blend is weakened and the modulus is mainly determined by the PVDF-PMMA phase, which results in the decrease of the modulus of the sample. Due to the formation of a new PMMA region at the interface when very high content of PMMA (40 wt%) is present in the sample, the contribution of PMMA becomes more apparent, which results in the slight enhancement of the sample modulus.

However, it is worth noting that although adding a mutually miscible third component is a very nice approach to compatibilize the immiscible polymer blends, the quantity of the third polymer demanded is often quite large, which is apparently different from the action of block copolymers in the immiscible polymer blends. In the latter system, a few amount of copolymers (usually smaller than 5 wt%) can exhibit apparent compatibilizing effect. The difference in the compatibilizing effects of the mutually miscible third component and block copolymer is possibly related to the different compatibilizing mechanisms.[67] Further work needs to be done to compare the compatibilizing effects of PMMA and other compatibilizer (block or graft copolymer) on the immiscible PLLA/PVDF blends.

4. CONCLUSIONS

In summary, the interaction in the immiscible PLLA/PVDF blend is successfully adjusted by adding a mutually miscible third component, i.e. PMMA. The interfacial tension measurements show that PMMA exhibits stronger interaction with PVDF, which results in more PMMA merging together with PVDF component during the melt-compounding processing. There is a competition effect between PLLA and PVDF when they absorb PMMA. In this condition, the interaction

between PLLA and PVDF can be improved at appropriate PMMA contents. Specifically, a part of PLLA (or PVDF) is carried into PVDF (or PLLA) component by PMMA, forming the interesting occlusion structure. However, at very high content of PMMA (40 wt%), the competition effect promotes PMMA to form a new region at the interface between PLLA and PVDF, and the PMMA region even shows the similar glass transition to that of pure PMMA. The mechanical properties measurements show that at appropriate PMMA contents (20-30 wt%), the ternary blends exhibit excellent fracture toughness. The enhanced interactions between components and the formation of the interesting occlusion structure are suggested to be the main toughening mechanisms. This work demonstrates that the microstructure and mechanical properties of the immiscible polymer blends can be adjusted by adding a mutually miscible third polymer via the competition mechanism.

AUTHOR INFORMATION

Corresponding author:

*TEL: +86 28 87603042. E-mail: yongwang1976@163.com

Notes

The authors declare no competing financial interests.

ACKNOWLEDGEMENTS

REFERENCES

(1) H. Bai, C. Huang, H. Xiu, Y. Gao, Q. Zhang and Q. Fu, *Polymer*, 2013, **54**, 5257-5266.

(2) H. Liu, W. Song, F. Chen, L. Guo, and J. Zhang, *Macromolecules*, 2011, **44**, 1513-1522.

(3) M. L. Robertson, K. Chang, W. M. Gramlich, and M. A. Hillmyer, *Macromolecules*, 2010, **43**,

1807-1814.

(4)   H. Xiu, C. Huang, H. Bai, J. Jiang, F. Chen, H. Deng, K. Wang, Q. Zhang, and Q. Fu, *Polymer*, 2014, **55**, 1593-1600.

(5)   P. Pötschke, and D. R. Paul. J. Macromol. Sci. Part C: Polym. Rev., 2003, **C43**, 87-141.

(6)   J. Chen, Y. Shen, J.-h. Yang, N. Zhang,;T. Huang, Y. Wang, and Z.-w. Zhou, *J. Mater. Chem. C*, 2013, **1**, 7808-7811.

(7)   A. Göldel, A. Marmur, G. R. Kasaliwal, P. Pötschke, and G. Heinrich, *Macromolecules,* 2011, **44**, 6094-6102.

(8)   J. Chen, Y.-y. Shi, J.-h. Yang, N. Zhang, T. Huang, C. Chen, Y. Wang, and Z.-w. Zhou, *J.Mater. Chem.*, 2012, **22**, 22398-22404.

(9)   J. Du, S. R. Armstrong, and E. Baer, *Polymer*, 2013, **54**, 5399-5407.

(10) G. Zhang, E. Baer, and A. Hiltner, *Polymer*, 2013, **54**, 4298-4308.

(11) G. T. Offord, S. R. Armstrong, B. D. Freeman, E. Baer, A. Hiltner, and D. R. Paul, *Polymer*, 2014, **55**, 1259-1266.

(12) J. M. Carr, M. Mackey, L. Flandin, A. Hiltner, and E. Baer, *Polymer*, 2013, **54**, 1679-1690.

(13) Y. Li, and H. Shimizu, *Macromolecules*, 2008, **41**, 5339-5344.

(14) W. Dong, X. Cao, and Y. Li, *Polym. Int.* 2013, In press. DOI: 10.1002/pi.4618.

(15) J. U. Schierholz, and G. P. Hellmann, *Polymer*, 2003, **44**, 2005-2013.

(16) T. Tanabe, H. Furukawa, and M. Okada, *Polymer*, 2003, **44**, 4765-4768.

(17) J. K. Lee, and C. D. Han, *Polymer*, 1999, **40**, 6277-6296.

(18) Z. H. Liu, Ph. Marechal, and R. Jérôme, *Polymer*, 1998, **39**, 1779-1785.

(19) H. J. Kim, K. J. Lee, and Y. Seo, *Macromolecules*, 2002, **35**, 1267-1275.

(20) G. A. Buxton, and A. C. Balazs, *Macromolecules*, 2005, **38**, 488-500.

(21) S. H. Anastasiadist, I. Gancarz, J. T. Koberstein, *Macromolecules*, 1989, **22**, 1449-1453.

(22) C.-H. Ho, C.-H. Wang, C.-I. Lin, and Y.-D. Lee, *Polymer*, 2008, **49**, 3902-3910.

(23) J. M. Machado, and C. S. Lee, *Polym. Eng. Sci.*, 1994, **34**, 59-68.

(24) H. Zhang, W. Guo, Y. Yu, B. Li, and C. Wu, *Eur. Polym. J.*, 2007, **43**, 3662-3670.

(25) M. Noureddin, and R. Jérôme, *Polymer*, 1999, **40**, 3919-3932.

(26) T. K. Kwei, H. L. Frisch, W. Radigan, and S. Vogel, *Macromolecules*, 1977, **10**, 157-160.

(27) C. J. T. Landry, *Polymer*, 1991, **32**, 44-52.

(28) B. Ameduri, and R. E. Prud'homme, *Polymer*, 1988, **29**, 1052-1057.

(29) N. Stathis, K. Dionissia, D. Sotiropoulou, J. K. Kallitsis, and N. K. Kalfoglou, *Polymer*, 1991,

32, 66-72.

(30) P. P. Lizymol, and S. Thomas, *J. Appl. Polym. Sci.*, 1994, **51**, 635-641.

(31) P. P. Lizymol, S. Thomas, and M. Jayabalan, Eur. Polym. J., 1997, **33**, 1397-1399.

(32) P. P. Lizymol, S. Thomas, and M. Jayabalan, Polym. Int., 1997, **44**, 23-29.

(33) P. P. Lizymol, and S. Thomas, J. Mater. Sci. Lett., 1998, **17**, 507-510.

(34) L. T. Lim, R. Auras, and M. Rubino, *Prog. Polym. Sci.*, 2008, **33**, 820-852.

(35) R. P. John, K. M. Nampoothiri, and A. Pandey, *Process Biochem.*, 2006, **41**, 759-763.

(36) R. E. Drumright, P. R. Gruber, and D. E. Henton, *Adv. Mater.*, 2000, **12**, 1841-1846.

(37) A.J. Nijenhuis, E. Colstee, D.W. Grijpma, and A. J. Pennings, *Polymer*, 1996, **37**, 5849-5857.

(38) A. M. Gajria, V. Davé, R. A. Gross, and S. P. McCarthy, *Polymer*, 1996, **37**, 437-444.

(39) J. W. Park, and S. S. Im, *Polymer*, 2003, **44**, 4341-4354.

(40) J. L. Eguiburua, J. J. Iruina, M. J. Fernandez-Berridia, and J. S. Románb, *Polymer*, 1998, **39**,

6891-6897.

(41) T. Shirahase, Y. Komatsu, Y. Tominaga, S. Asai, and M. Sumita, *Polymer*, 2006, **47**, 4839-4844.

(42) Y. Ding, P. Zhang, Z. Long, Y. Jiang, F. Xu, and W. Di, *Sci. Technol. Adv. Mater.*, 2008, **9**, 015005-015008.

(43) D. Xiang, N.N. Hsu, and G. V. Blessing, *Ultrasonics*, 1996, **34**, 641-647.

(44) H. Sasaki, P. K. Bal, H. Yoshid, and E. Ito, *Polymer*, 1995, **36**, 4805-4810.

(45) Y. J. Li, Y. Iwakura, and H. Shimizu, *Macromolecules*, 2008, **41**, 3396-3400.

(46) T. Wang, H. Li, F. Wang, S. Yan, and J. M. Schultz, *J. Phys. Chem. B*, 2011, **115**, 7814-7822.

(47) Z. b. Qiu, C. Z. Yan, J. M. Lu, and W. Yang, *Macromolecules*, 2007, **40**, 5047-5053.

(48) J. Liu, Z. Qiu, and B.-J. Jungnickel, *J. Polym. Sci. Part B: Polym. Phys.*, 2005, **43**, 287-295.

(49) P. Pan, G. Shan, and Y. Bao, *Ind. Eng. Chem. Res.*, 2014, **53**, 3148-3156.

(50) Q. Xie, K. Ke, W. -R Jiang, W. Yang, Z. –Y. Liu, B. –H. Xie, and M.-B. Yang, *J. Appl. Polym. Sci.*, 2013, **129**, 1686-1696.

(51) A. Kaito, Y. Iwakura, Y. Li, and H. Shimizu, *J. Polym. Sci. Part B: Polym. Phys.*, 2008, **46**, 1376-1389.

(52) F. Fowkes, *J. Phys. Chem.*, 1962, **66**, 382.

(53) D. K. Owens, and R. Wendt, *J. Appl. Polym. Sci.*, 1969, **13**, 1741-1747.

(54) S. Wu, *Polymer interface and adhesion*. M. Dekker, New York, 1982.

(55) E. N. Dalal, *Langmuir*, 1987, **3**, 1009-1015.

(56) S. Ravati, and B. D. Favis, *Polymer*, 2010, **51**, 3669-3684.

(57) R. E. Neuendorf, E. Saiz, A.P. Tomsia, and R. O. Ritchie, *Acta Biomater.,* 2008, **4**, 1288-1296.

(58) I. Elashmawi, and N. Hakeem, *Polym. Eng. Sci.*, 2008, **48**, 895-901.

(59) H. M. Chen, J. Chen, L. N. Shao, J. H. Yang, T. Huang, N. Zhang, and Y. Wang, *J. Polym. Sci. Part B: Polym. Phys.*, 2013, **51**, 183-196.

(60) B.-E. El Mohajir, and N. Heymans, *Polymer*, 2001, **42**, 5661-5667.

(61) A. M. Harris, and E. C. Lee, *J. Appl. Polym. Sci.*, 2008, **107**, 2246-2255.

(62) D.-J. Lin, C.-L. Chang, C.-K. Lee, and L.-P. Cheng, *Eur. Polym. J.*, 2006, **42**, 2407-2418.

(63) S.-I. Hirota, T. Sato, Y. Tominaga, S. Asai, and M. Sumita, *Polymer*, 2006, **47**, 3954-3960.

(64) C. Samuel, J.-M. Raquez, and P. Dubois, *Polymer*, 2013, **54**, 3931-3939.

(65) Y. Lin, H. B. Chen, C. M. Chan, and J. S. Wu, *Macromolecules*, 2008, **41**, 9204-9213.

(66) G. -X. Wei, H. –J. Sue, J. Chu, C. Huang, and K. Gong, *Polymer*, 2000, **41**, 2947-2960.

(67) C. Koning, M. V. Duin, C. Pagnoulle, and R. Jerome, *Prog. Polym. Sci.*, 1998, **23**, 707-757.

Table 1. Contact angle between distilled water, methylene iodide and polymer surfaces

Component	Distilled water	Methylene iodide
PVDF	80.2	43.1
PLLA	75.1	41.1
PMMA	78.7	26.8

Table 2. Surface energy data of component.

Component	γ (mJ/m^2)	γ^d (mJ/m^2)	γ^p (mJ/m^2)	Temperature dependence $(-d\gamma/dT)$ (mJ·m^{-2}·℃$^{-1}$)	Ref.
PVDF	29.4	25.9	3.5	0.057	[50]
PLLA	32.5	27.3	5.2	0.05	[51]
PMMA	33.2	30.9	2.3	0.076	[50]

Table 3. Interfacial tensions as calculated using Harmonic and Geometric mean equations. The data refer the interfacial tensions at melt temperature of 185 °C.

Component couple	Interfacial tension	
	Based on Harmonic-mean equation (mJ/m^2)	Based on Geometric -mean equation (mJ/m^2)
PVDF-PMMA	0.69	0.35
PLLA-PMMA	1.34	0.69

Figure captions:

Figure 1: Mechanical loss factor of the binary blends obtained from DMA measurement.

Figure 2: Mechanical loss factor of the ternary blends obtained from DMA measurement. For making a comparison, the result of the binary PLLA/PVDF (60/40) blend is also shown.

Figure 3: Schematic representations showing the interactions between components and the corresponding mechanical loss factor.

Figure 4: WAXD profiles showing the crystalline structures of all the samples.

Figure 5: DSC heating curves showing the cold crystallization and melting behaviors of the components

Figure 6: The variations of complex viscosity of PLLA, PVDF, and PMMA obtained from rheological measurement.

Figure 7: SEM images showing the morphological changes of the binary (a) and ternary blends (b-e) with different PMMA contents. (a) the binary PLLA/PVDF (60/40) blend, (b) PLLA/PVDF/PMMA (60/40/10), (c) PLLA/PVDF/PMMA (60/40/20), (d) PLLA/PVDF/PMMA (60/40/30) and (e) PLLA/PVDF/PMMA (60/40/40)

Figure 8: TEM images showing the morphologies of the ternary PLLA/PVDF/PMMA (60/40/30) blend obtained at low (left) and high (right) magnifications.

Figure 9: (a) The representative engineering stress-strain curves of all the samples and (b, c) the variations of the corresponding tensile properties versus the content of PMMA.
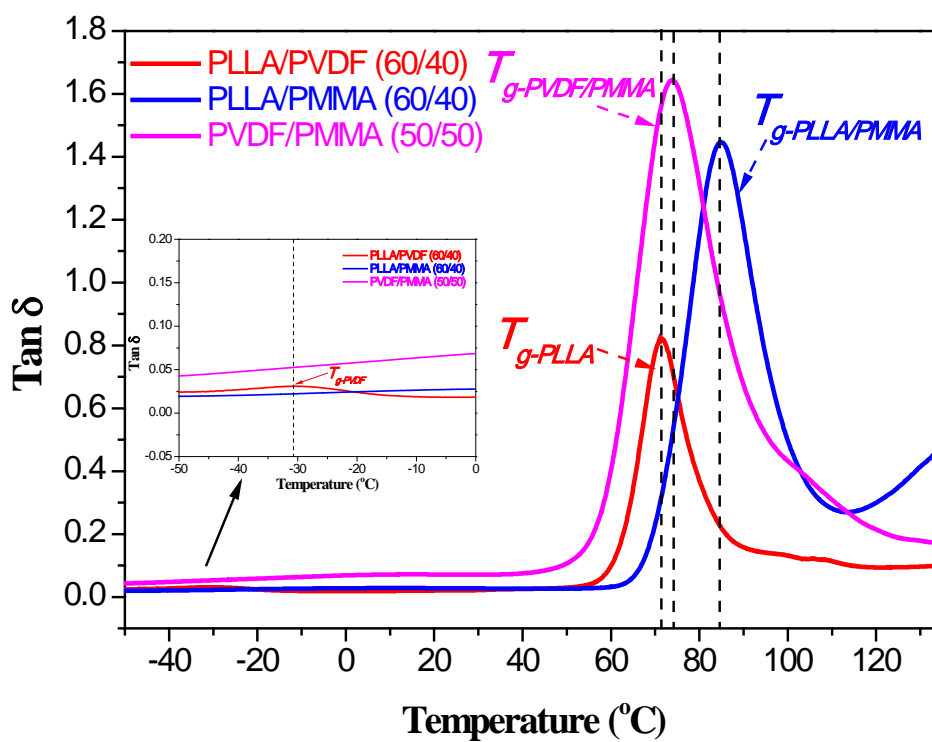
Figure 1
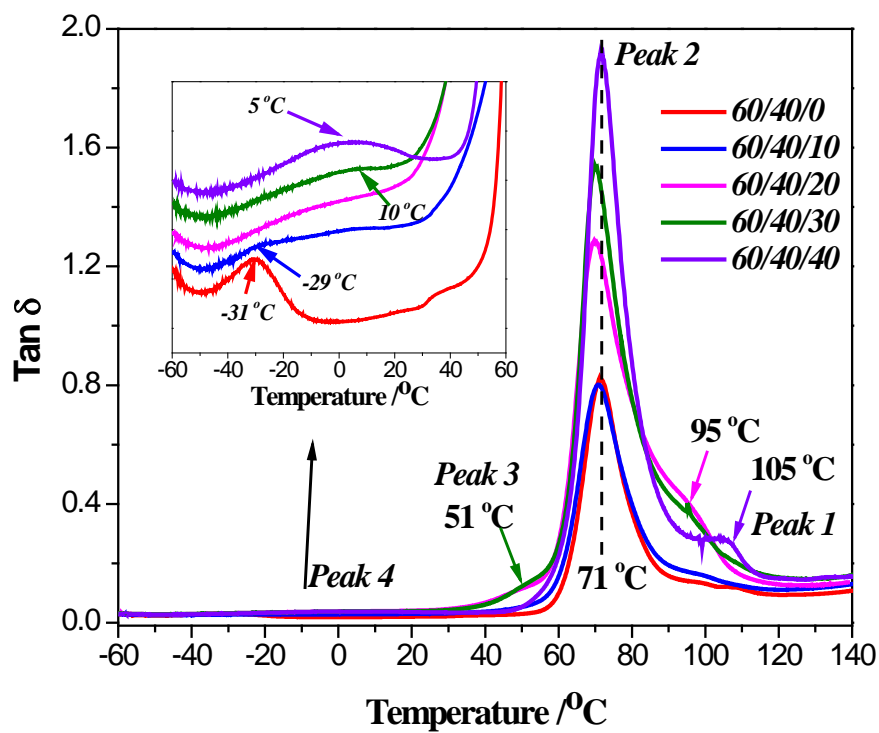
Figure 2
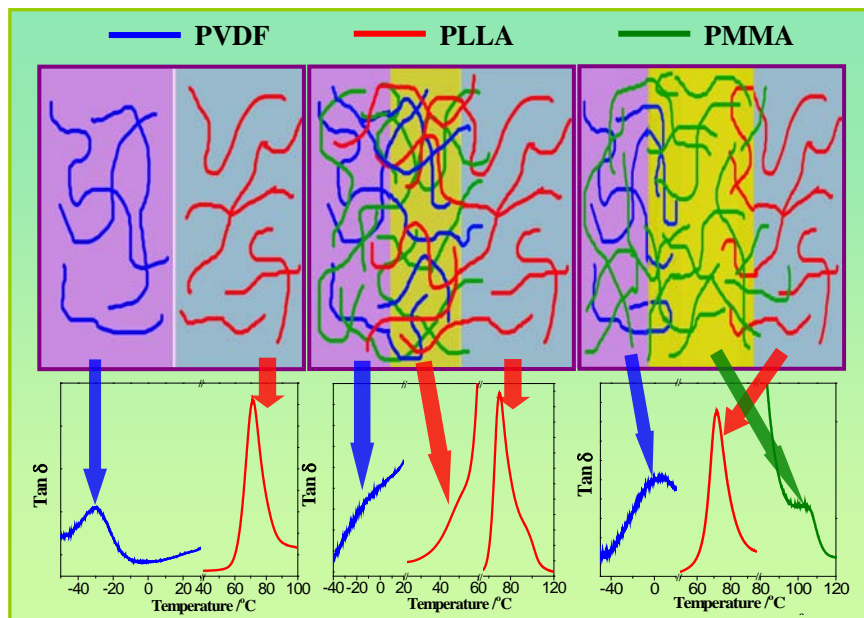
Figure 3
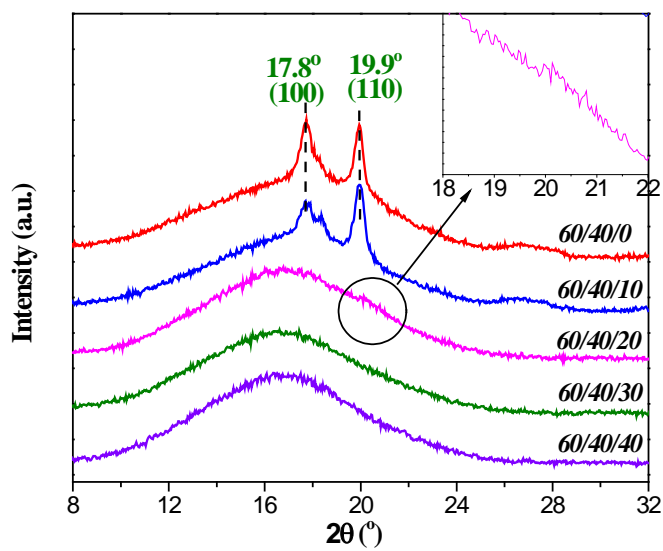
Figure 4
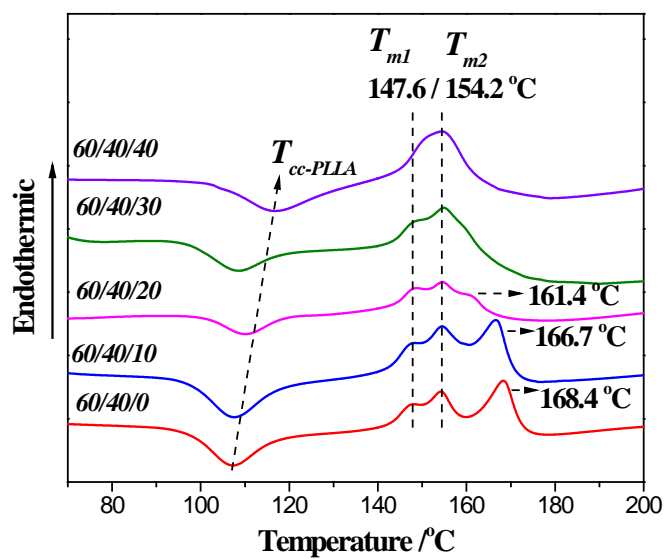
Figure 5

Figure 6

Figure 7

30
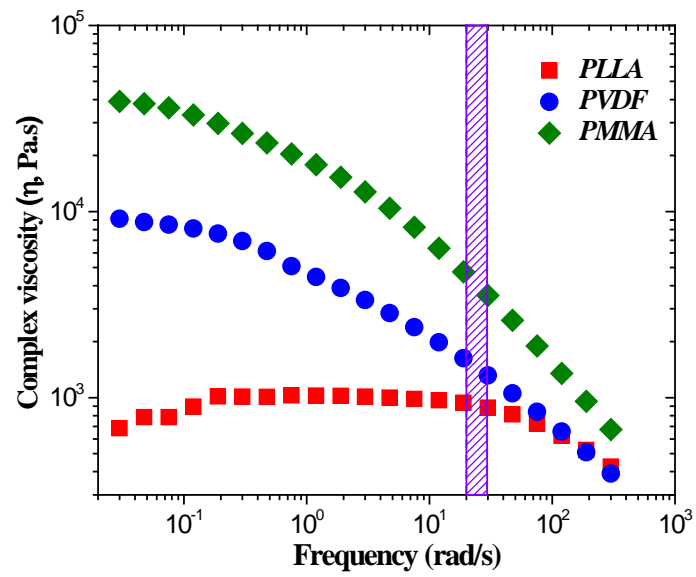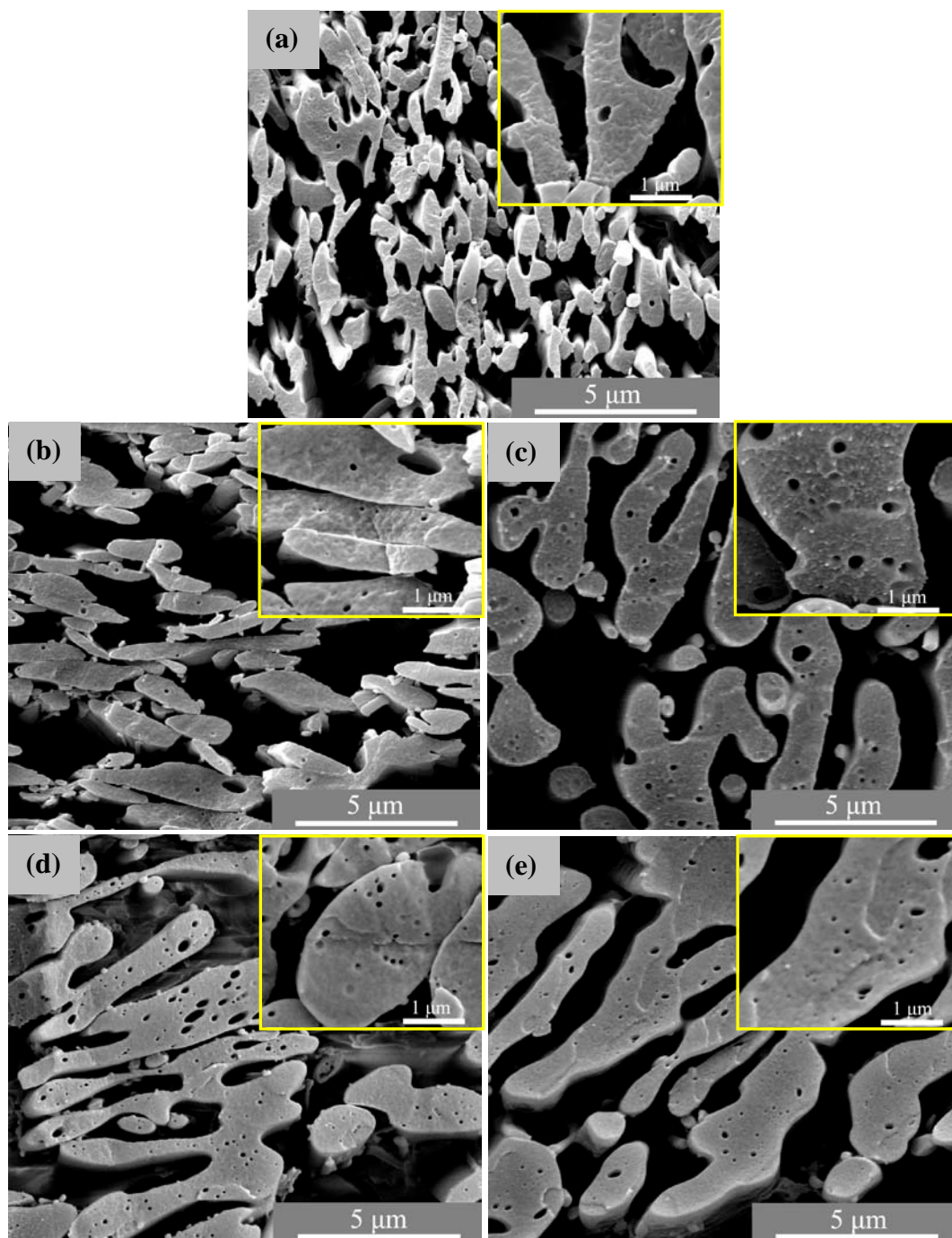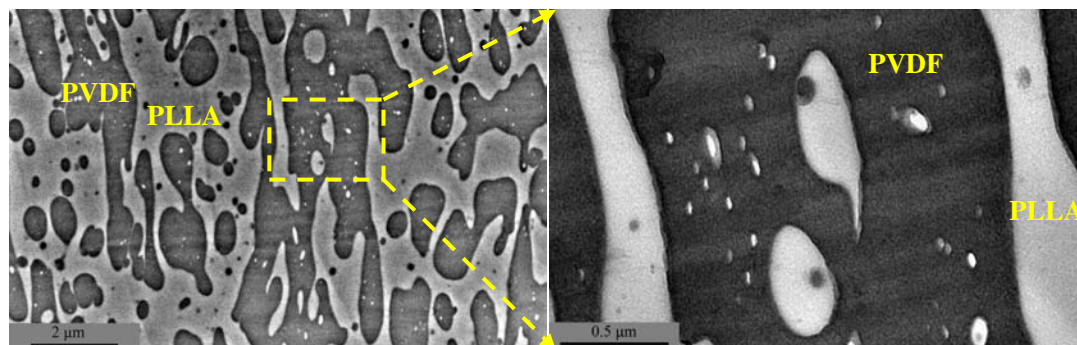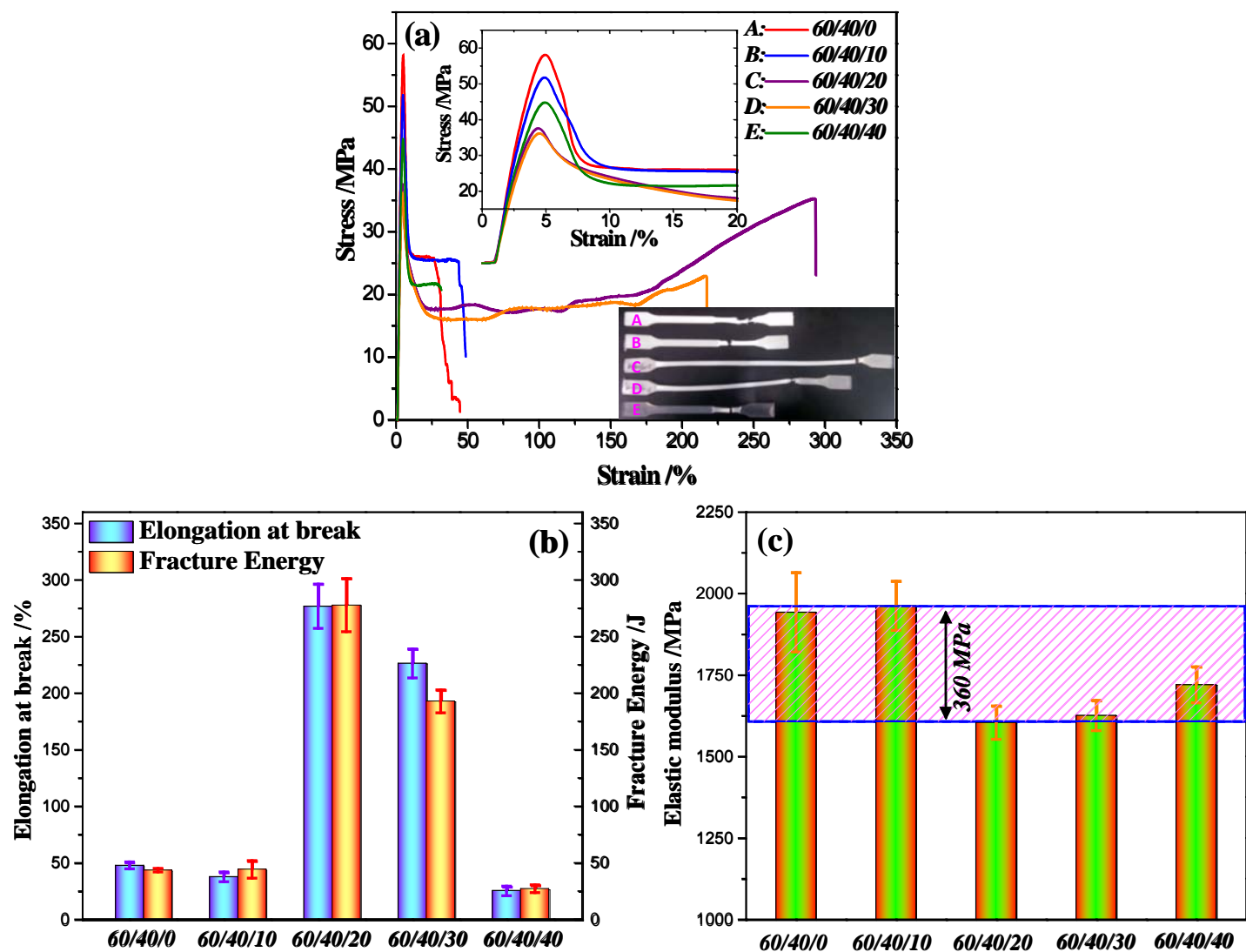
Figure 8

Figure 9

Table of Content use only

Tuning Interaction of Immiscible Poly(L-lactide)/Poly(vinylidene fluoride) Blend by Adding Poly(methyl methacrylate) via a Competition Mechanism and the Resultant Mechanical Properties

Hai-ming Chen, Xiong-fei Wang, Dan Liu, Yang-peng Wang, Jing-hui Yang, Yong Wang, Chao-liang Zhang, Zuo-wan Zhou
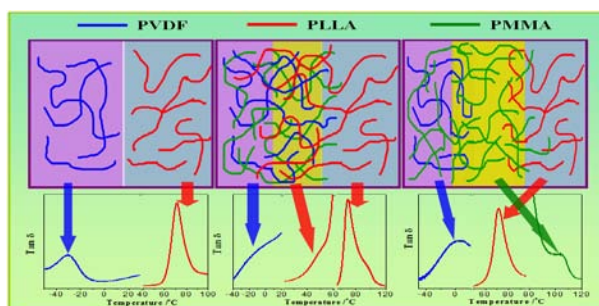
Through improving the interaction and forming the occlusion structure, largely improved ductility is achieved by adding PMMA into PLLA/PVDF blend.